JOURNAL OF SPACECRAFT AND ROCKETS
Vol. 47, No. 1, January–February 2010

First Korea Space Launch Vehicle Kick Motor Movable Nozzle Motion

Jae-Seok Yoo*
Korea Aerospace Research Institute, Daejeon 305-333, Republic of Korea

DOI: 10.2514/1.44921

In this study, nozzle rotational angle was obtained from measuring axial displacements from displacement gauges. Compensation equations for offaxis and slip effects of the displacement gauge were newly developed to obtain the nozzle rotational angle. A thrust vector control stroke test was conducted to provide linear coefficients related to pitch, yaw, and inclinometer angles with respect to the thrust vector control input voltage. The convergence of the compensation equations was satisfied with a percent relative error, which was under 0.0004%. From the compensation equations and the linear coefficients, the nozzle rotational angle history was accurately obtained in the thrust vector control scenario test within 0.01 deg. However, there was an offset in the rotational angle in the ground firing tests. This offset was within the maximum 0.04 deg, and it was caused by the deformation of the end position of the support beam, which was induced by combustion pressure.

Nomenclature

D	=	projected distance of each displacement gauge as shown in Fig. 1 (right-hand side), mm
$E_{ai.\text{pitch}}$	=	ith percent relative error for the compensated pitch rotational angle, %
$E_{ai.\text{yaw}}$	=	ith percent relative error for the compensated yaw rotational angle, %
$L_{\text{INCL}-P}$	=	linear coefficient of the inclinometer angle for the thrust vector control input voltage on pitch actuating, deg /V
$L_{\text{INCL}-Y}$	=	linear coefficient of the inclinometer angle for the thrust vector control input voltage on yaw actuating, deg /V
L_{P-P}	=	linear coefficient of the calculated pitch angle for the thrust vector control input voltage on pitch actuating, deg /V
L_{P-Y}	=	linear coefficient of the calculated pitch angle for the thrust vector control input voltage on yaw actuating, deg /V
L_{Y-P}	=	linear coefficient of the calculated yaw angle for the thrust vector control input voltage on pitch actuating, deg /V
L_{Y-Y}	=	linear coefficient of the calculated yaw angle for the thrust vector control input voltage on yaw actuating, deg /V
$\text{Pitch}_{\text{Comp}.i}$	=	ith compensated pitch rotational angle, deg
$\text{Pitch}_{\text{Disp}.i.}$	=	ith compensated pitch rotational angle with only offaxis effect, deg
$\text{Yaw}_{\text{Comp}.i}$	=	ith compensated yaw rotational angle, deg
$\text{Yaw}_{\text{Disp}.i.}$	=	ith compensated yaw rotational angle with only offaxis effect, deg
$\Delta\text{disp}_{\text{Pitch}}$	=	displacement difference of 346 and 166 deg displacement gauge, mm
$\Delta\text{disp}_{\text{Yaw}}$	=	displacement difference of 76 and 256 deg displacement gauge, mm

Received 14 April 2009; revision received 9 September 2009; accepted for publication 10 September 2009.

*Senior Researcher, Structures and Materials Department; jsyoo@kari.re.kr.

I. Introduction

IN THE developing test of the first Korea Space Launch Vehicle (KSLV-1) kick motor nozzle, in which a flexible seal was assembled, the nozzle moved by thrust vector control (TVC). The TVC actuating scenario was developed to study the dynamic performance and control accuracy of the nozzle, which was related to the coincidence of TVC command, actual response of the rotational angle, and TVC command and feedback frequency. The TVC accuracy and dynamic performance are directly connected to the successful launch of a satellite. To evaluate and improve the TVC accuracy and dynamic performance, the accurate measurement of the nozzle rotational angle and frequency are very important.

Generally, it is hard to measure the rotational angle by using an inclinometer (which is a kind of gravity sensor in the TVC scenario and ground firing test) because of a high level of vibration and high frequency TVC response. However, it is possible to obtain the nozzle rotational angle by using a displacement gauge, which consists of four strain gauges (full-bridge connection) in the TVC scenario and the ground firing test.

Ishibashi et al. [1] developed a design, development, and flight test for the H-II solid rocket booster TVC system. The end position of the TVC actuator was fixed at the inner root of the rear skirt of the motor case, similar to the space shuttle solid rocket booster [2]. The actuator performance was verified in the development and flight test. However, a detailed comparison of the TVC command and feedback was not represented. Ellis [3] researched the design, fabrication, and testing of a supersonic splitline flexible nozzle, which is an unsubmerged nozzle. The end position of the TVC actuator is fixed at the rear boss of the motor case. In the ground firing test, the TVC actuator rotated the nozzle up to 5 deg. Also, the TVC command and feedback are coincident each other. However, this is not a flight model but a subscale and heavy type model because of the conservatism of the concept design. Akiba et al. [4] developed the M-3SII vehicle, which is assembled with a movable nozzle. The nozzle moves in only one direction. In a ground firing test, there was a problem of the offset angle of the movable nozzle caused by the chamber pressurization. By employing a reference potentiometer at the opposite side of two servo actuators and feeding back the signal from the potentiometer, the offset problem was solved. The servo actuator and the reference potentiometer strokes are not linear. The offset angle was measured by two dial gauges. The offset angle is satisfied within 0.1 deg, which is the requirement of the nozzle. However, the accuracy of the offset angle measured by the dial gauges was not represented. Carnevale and Resta [5] developed the new Vega TVC subsystem. The step response of the Z23 TDM (TVC development model) matches well with the reference signal, but the Z9 TDM has an important static error that is likely due to a signal saturation occurring in the external

linear variable differential transformer rather than the thrust function itself.

Knauber [6] described the major sources of thrust misalignment of fixed-nozzle solid rocket motors that are caused by manufacturing mechanical tolerances, motor case distortions, and nozzle cant angles, as a result of pressurization, etc. Also in this reference, changes in motor case and nozzle deflections as a result of pressurization were both measured in a hydrotest and static firing, using deflectometers and strain gauges. However, detailed methods of measuring the nozzle and motor case deflection and the processing of measured data were not represented.

In the preceding references, the couple effect between the TVC actuators was not studied. Furthermore, the detailed TVC accuracy and the calculation method for the nozzle rotational angle by gauges were not represented.

In this study, the compensation equations for the offset and offaxis effects were newly developed to obtain the accurate nozzle rotational angle calculated from the measured axial displacements by the displacement gauges. In addition, the detailed method to obtain the accurate nozzle rotational angle was represented. The TVC stroke test was done to provide the linear coefficients, which are used for the calculation of the nozzle rotational angle. The compensation equations were verified by the TVC scenario test. Also, the nozzle rotational angles by the displacement gauges were successfully measured in the ground firing tests.

II. Configuration

In the KSLV-1 kick motor system, shown in Fig. 2, the support position of the TVC actuator is far from the hard point, which is the connecting part of the rear boss of the combustion chamber and the nozzle connecting part (similar to the TVC nozzle of Star 48B [7] and the Indian Space Research Organization's solid rocket nozzle [8]). This kind of TVC actuator support beam is largely deformed by the rotational deformation of the mounting roots of the support beam induced by combustion pressure. To evaluate the differences between the TVC command and the feedback data by the deformation of the support beam, it is important to measure the accurate nozzle rotational angle, excluding the rotational angle by the deformation of the TVC support beam. Therefore, the displacement gauges were

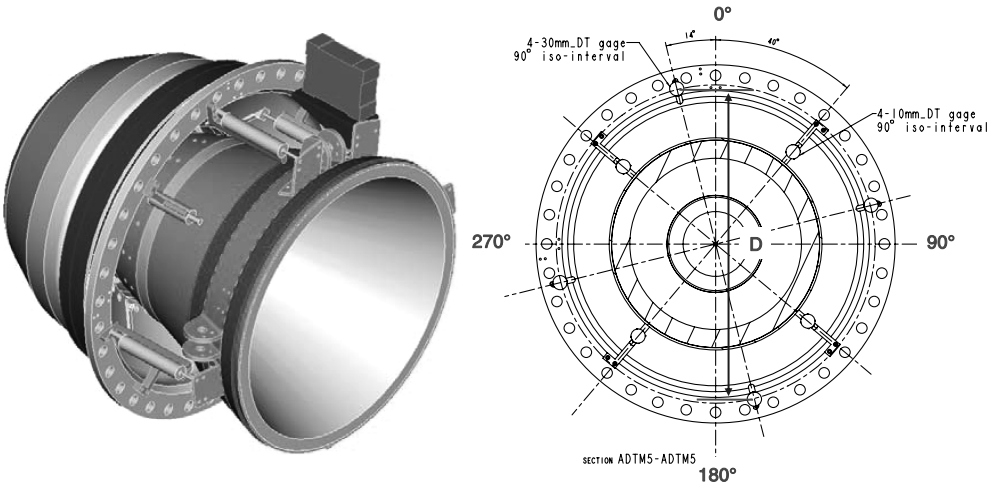

Fig. 1 Installation position of displacement gauges (DT denotes displacement).

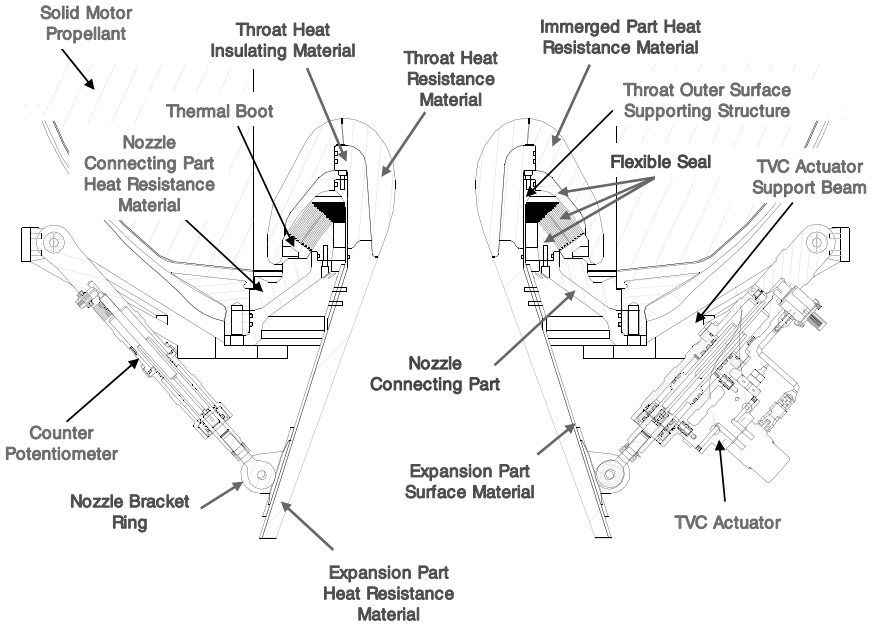

Fig. 2 Kick motor configuration.

installed at the hard point, which is the joining plane of the nozzle and combustion chamber, as shown in Fig. 1. The measurement of the axial displacement of the nozzle, which is mainly generated by the deformation of the rubber layers of flexible seal, is also important in evaluating the margin of the effective stroke of the TVC actuator.

During the ground firing test, because of the deformation of the support position by the TVC actuation force and the combustion pressure, there was some error in the TVC feedback data measured by the TVC actuator and the counter potentiometer. Moreover, the installation angle of the TVC actuators are identically orthogonal. However, when the TVC actuators move, there is interference between each actuator in the real situation, which also generates TVC feedback error.

In this paper, to investigate the TVC accuracy under the TVC actuation force and the combustion pressure, the displacement gauges (which have a 30 mm effective stroke and 0.01 mm accuracy and resolution) were installed at the hard point. To avoid interference with the TVC actuators, the installation position of the displacement gauges is inevitably 14 deg offdirection with respect to the pitch and yaw direction. When each actuator moves to the pitch and yaw direction, the interference of the each displacement gauge by the offaxis installation position is automatically generated. Furthermore, for the compensation of the nozzle rotational angle calculated from measured displacements, an inclinometer was used, as shown in Fig. 3.

III. Thrust Vector Control Stroke Test

Figure 4 shows the total number of steps to obtain the nozzle rotational angle from measured displacements in the TVC scenario and the ground firing test. The TVC stroke test was conducted to gain linear coefficients from measured displacements. During the TVC stroke test, the TVC actuator slowly rotates the nozzle within a ± 1.5 deg range in the pitch (0–180 deg) and yaw (90–270 deg) direction, as shown in Fig. 5. The displacements and the inclinometer angle are also measured at the same time. The inclinometer that is used in this TVC stroke test has 0.001 deg resolution and guarantees under $1/60$ deg accuracy.

Figure 3 shows the installation of the TVC actuator, the inclinometer, and the displacement gauges. After the TVC stroke test (± 1.5 deg), the inclinometer is removed in the TVC scenario test. The inclinometer, which is a kind of a gravity sensor, is not appropriate for measuring the dynamic rotational angle during the TVC scenario and the ground firing test.

First, the TVC stroke test (± 1.5 deg) is conducted in the pitch direction, and the pitch actuator only moves the nozzle slowly from -3 to 3 deg. After the TVC stroke test is done in the pitch direction, the kick motor is rotated 90 deg clockwise to measure the angle by inclinometer when we see the kick motor in the rear. After the rotation of the kick motor, the TVC stroke test (± 1.5 deg) is executed in the yaw direction. The nozzle displacements in the pitch direction for the TVC stroke test are measured, and shown in Fig. 5 (left-hand side). The nozzle displacements at 346 and 166 deg, which are close to the pitch direction (0–180 deg), are larger than those at 76 and 256 deg.

By these measured nozzle displacements, the pitch and yaw nozzle rotational angle can be calculated by Eq. (1), which is shown next:

$$\begin{aligned} \text{Pitch}_{\text{Disp.0}} &= \tan^{-1}\left(\frac{\Delta \text{disp}_{\text{Pitch}}}{D}\right); \\ \text{Yaw}_{\text{Disp.0}} &= \tan^{-1}\left(\frac{\Delta \text{disp}_{\text{Yaw}}}{D}\right) \end{aligned} \tag{1}$$

The calculated nozzle rotational angle in Eq. (1) is shown in Fig. 5 (right-hand side). Because the displacement gauges are installed at the 14 deg offaxis position from the pitch or yaw direction, as shown in Fig. 1, all displacements of the gauges are measured in the pitch or

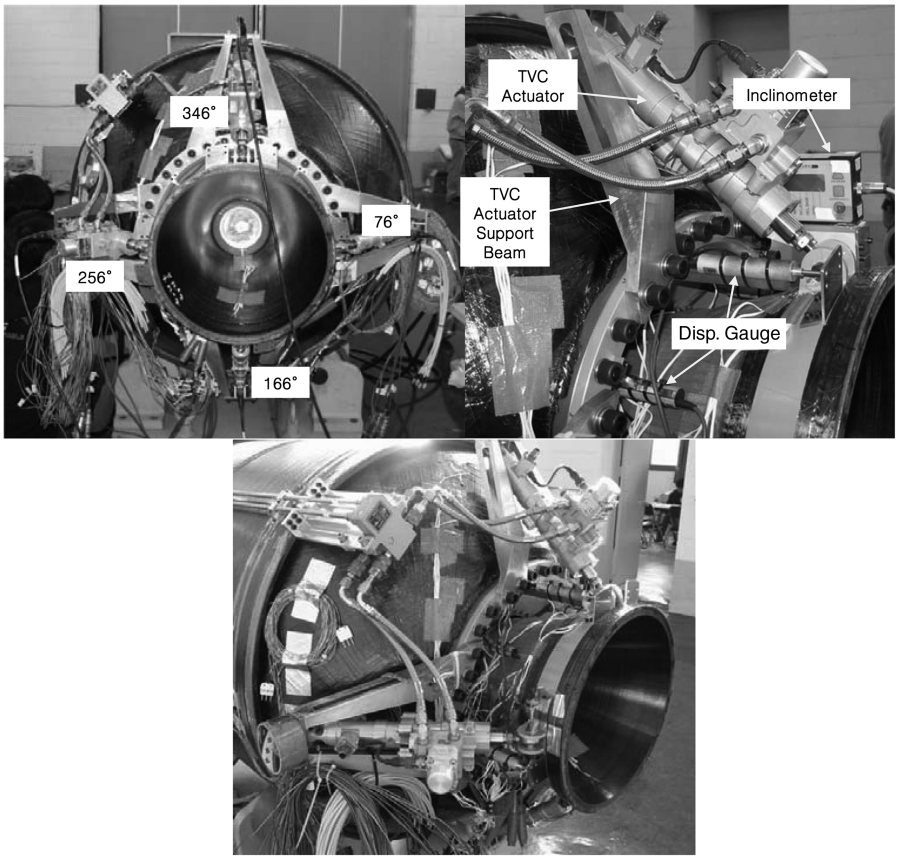

Fig. 3 Displacement gauge installation pictures.

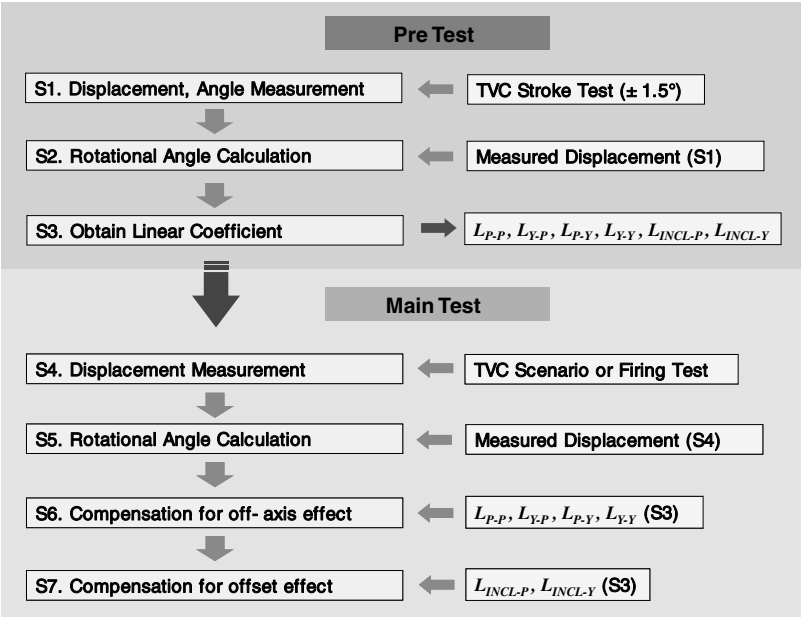

Fig. 4 Total steps to obtain nozzle rotational angle from measured displacement.

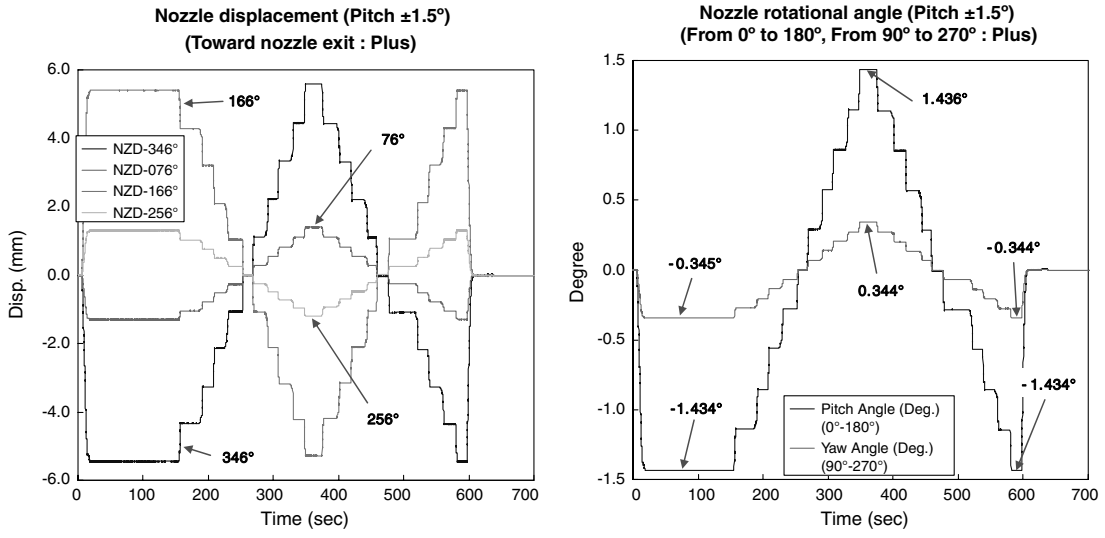

Fig. 5 Nozzle displacement (NZD) and calculated rotational angle for ±1.5 deg pitch TVC stroke test.

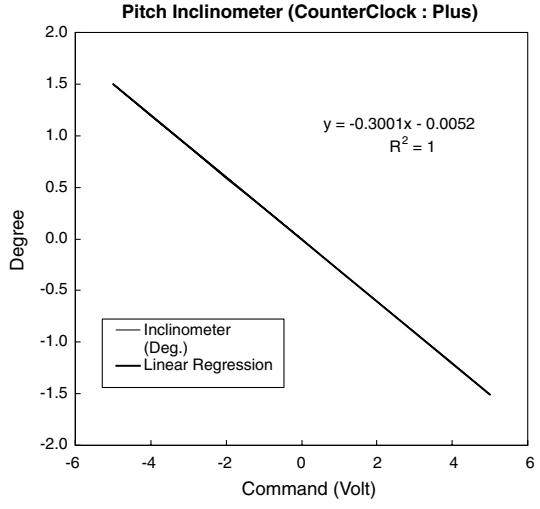

Fig. 6 Inclinometer angle history for ±1.5 deg pitch TVC stroke test.

yaw TVC stroke test. During the TVC stroke test in the pitch direction, the nozzle rotational angle (calculated by the displacements measured at 76 and 256 deg near the yaw direction) is about 24% of the nozzle rotational angle calculated by the displacements measured at 346 and 166 deg near the pitch direction.

There is a difference with the calculated rotational angle and the inclinometer angle, as shown in Tables 1 and 2. As the rotational angle becomes larger, the difference of the calculated rotational angle from the measured displacements and the inclinometer angle becomes larger because of the slide effect between the tip of displacement gauge and the displacement gauge bracket, as shown in Fig. 3. To compensate for the difference, the relation of the calculated rotational angle and the inclinometer angle is investigated, as shown in Figs. 6 and 7.

Because the TVC actuator is moved by the TVC input signal, the TVC input signal is selected as the reference signal. The TVC actuator rotates the nozzle by 0.3 deg per the TVC input signal voltage. There are linear relations among the angle from the inclinometer, the calculated pitch, and the yaw angle with respect to the TVC input signal. Therefore, the calculated rotational angle from the

Table 1 Inclinometer, pitch, and yaw angle in TVC stroke test during pitch stroke

TVC input signal, V	Inclinometer, deg	Pitch angle, deg (0–180 deg)	Yaw angle, deg (90–270 deg)
0	0.000	−0.001	0.000
−5	1.500	−1.434	−0.345
−4	1.193	−1.138	−0.273
−3	0.896	−0.855	−0.206
−2	0.585	−0.558	−0.135
−1	0.290	−0.277	−0.068
0	0.000	0.001	0.000
1	−0.306	0.290	0.070
2	−0.606	0.576	0.138
3	−0.905	0.860	0.204
4	−1.204	1.146	0.273
5	−1.508	1.436	0.344
4	−1.205	1.140	0.271
3	−0.905	0.854	0.202
2	−0.607	0.569	0.136
1	−0.307	0.284	0.068
0	0.000	−0.007	−0.001
−1	0.291	−0.283	−0.068
−2	0.590	−0.568	−0.138
−3	0.895	−0.858	−0.208
−4	1.195	−1.145	−0.276
−5	1.499	−1.434	−0.344
0	−0.001	−0.001	0.000

Table 2 Inclinometer, pitch, and yaw angle in TVC stroke test during yaw stroke

TVC input signal, V	Inclinometer, deg	Pitch angle, deg (0–180 deg)	Yaw angle, deg (90–270 deg)
0	0.000	0.001	0.000
−5	1.492	−0.338	1.419
−4	1.195	−0.271	1.136
−3	0.893	−0.202	0.849
−2	0.593	−0.135	0.562
−1	0.288	−0.064	0.273
0	−0.002	0.002	−0.004
1	−0.310	0.072	−0.297
2	−0.608	0.137	−0.580
3	−0.910	0.206	−0.867
4	−1.209	0.276	−1.152
5	−1.509	0.347	−1.439
4	−1.208	0.278	−1.152
3	−0.909	0.208	−0.868
2	−0.609	0.137	−0.581
1	−0.313	0.070	−0.299
0	0.001	0.000	0.000
−1	0.290	−0.064	0.275
−2	0.594	−0.133	0.564
−3	0.892	−0.202	0.849
−4	1.194	−0.271	1.136
−5	1.491	−0.337	1.418
0	−0.002	0.001	−0.003

measured displacements can be compensated accurately. Each linear coefficient about the TVC input signal is arranged in Table 3. The TVC stroke tests were done one or two times before the ground firing tests, as shown in Table 3.

IV. Compensation of Offaxis and Offset Effect

By the linear coefficients gained from the TVC stroke test (±1.5 deg) (the compensation of the offaxis and offset effects), which are the angle compensation from the inclinometer, the accurate nozzle rotational angle can be obtained in the TVC scenario test. The compensations of the offaxis and the offset effects are described next in detail.

If the TVC actuator moves only in the pitch or yaw direction, the calculated nozzle angle can be compensated accurately by multiplying the calculated rotational angle by $(L_{\mathrm{INCL}-P})/(L_{P-P})$ or $(L_{\mathrm{INCL}-Y})/(L_{Y-Y})$. However, when the TVC actuator moves in the pitch and yaw direction simultaneously, there is a couple effect between each displacement gauge, because the displacement gauge installation position is off with respect to the pitch and yaw direction, as shown in Fig. 1

$$\mathrm{Pitch}_{\mathrm{Comp.0}} = \mathrm{Pitch}_{\mathrm{Disp.0}} \times \frac{L_{\mathrm{INCL}-P}}{L_{P-P}};$$

$$\mathrm{Yaw}_{\mathrm{Comp.0}} = \mathrm{Yaw}_{\mathrm{Disp.0}} \times \frac{L_{\mathrm{INCL}-Y}}{L_{Y-Y}} \tag{2}$$

There is good agreement between the TVC scenario and the nozzle rotational angle compensated by Eq. (2) during the actuation in the only pitch direction, as shown in Fig. 8. Equation (2) ignores the offaxis effect of the displacement gauges. However, there is a difference between the TVC scenario and the nozzle rotational angle of Eq. (2) during the actuation in the pitch and yaw direction, simultaneously. In the only pitch actuation period, the yaw nozzle rotational angle is detected. as shown in Fig. 8 (right-hand side), due to the offaxis effect of displacement gauges.

To compensate the offaxis effect of the displacement gauges, compensation equations are developed, as shown next:

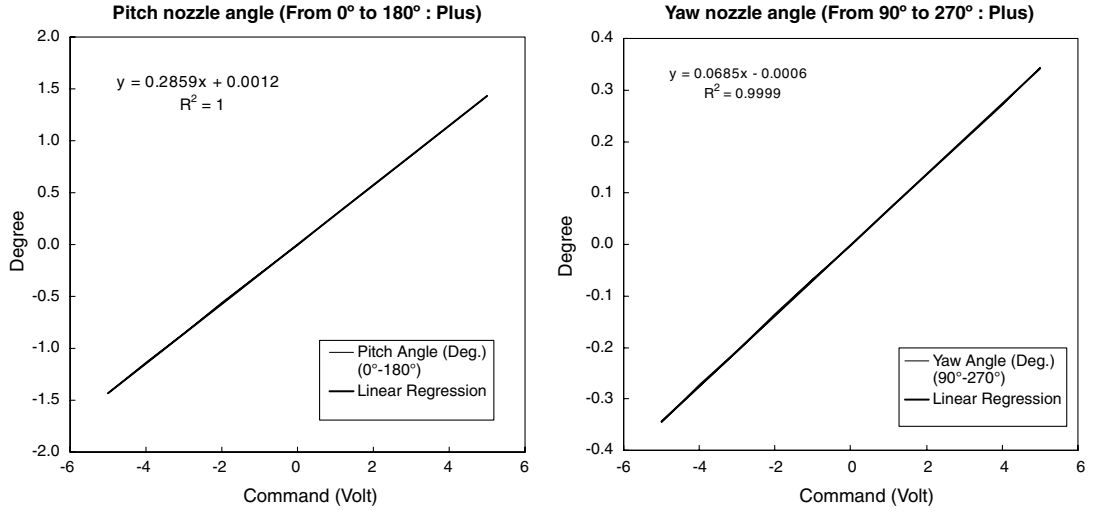

Fig. 7 Calculated nozzle rotational angle history for ±1.5 deg pitch TVC stroke test.

Table 3 Linear coefficients of pitch, yaw, and inclinometer angle for TVC input signal

GT	Test No./Average	Pitch stroke test, deg /V			Yaw stroke test, deg /V		
		L_{P-P}	L_{Y-P}	$L_{\mathrm{INCL}-P}$	L_{P-Y}	L_{Y-Y}	$L_{\mathrm{INCL}-Y}$
	No. 4	0.2886	0.0664	0.2997	0.0666	0.2886	0.3009
	Test 1	0.2857	0.0680	0.2998	0.0688	0.2857	0.3000
No. 5	Test 2	0.2859	0.0685	0.3001	0.0683	0.2859	0.3002
	Average	0.2858	0.0683	0.3000	0.0686	0.2858	0.3001
	Test 1	0.2882	0.0675	0.3003	0.0685	0.2908	0.3008
No. 6	Test 2	0.2894	0.0675	0.3005	0.0688	0.2909	0.2996
	Average	0.2888	0.0675	0.3004	0.0687	0.2909	0.3002
	Total average	0.2877	0.0674	0.3000	0.0679	0.2884	0.3004

$$\mathrm{Pitch}_{\mathrm{Disp}.i} = \mathrm{Pitch}_{\mathrm{Disp}.0} + \mathrm{Yaw}_{\mathrm{Disp}.i-1} \times \frac{L_{P-Y}}{L_{Y-Y}}, \qquad i = 1, 2, \cdots, 16;$$

$$\mathrm{Yaw}_{\mathrm{Disp}.i} = \mathrm{Yaw}_{\mathrm{Disp}.0} - \mathrm{Pitch}_{\mathrm{Disp}.i-1} \times \frac{L_{Y-P}}{L_{P-P}}, \qquad i = 1, 2, \cdots, 16 \tag{3}$$

In Eq. (3), the offaxis effect of the displacement gauges is accurately compensated for by increasing the iteration number. Because the value of $(L_{P-Y})/(L_{Y-Y})$ or $(L_{Y-P})/(L_{P-P})$ is about 0.23, as shown in Table 3, as the iteration progresses, the compensation of the pitch or yaw rotational angle converges rapidly.

After the compensation of the offaxis effect, the accurate nozzle angle can finally be obtained by Eq. (4), which is the compensation for the offset effect:

$$\mathrm{Pitch}_{\mathrm{Comp}.i} = \mathrm{Pitch}_{\mathrm{Disp}.i} \times \frac{L_{\mathrm{INCL}-P}}{L_{P-P}};$$

$$\mathrm{Yaw}_{\mathrm{Comp}.i} = \mathrm{Yaw}_{\mathrm{Disp}.i} \times \frac{L_{\mathrm{INCL}-Y}}{L_{Y-Y}} \tag{4}$$

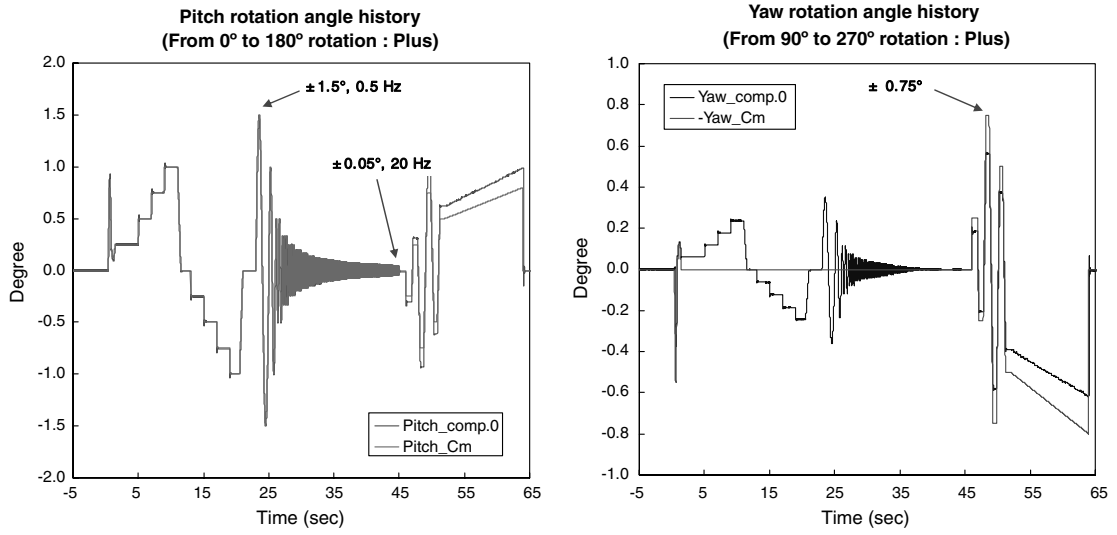

Fig. 8 Nozzle rotational angle history for TVC scenario test (only offset compensation).

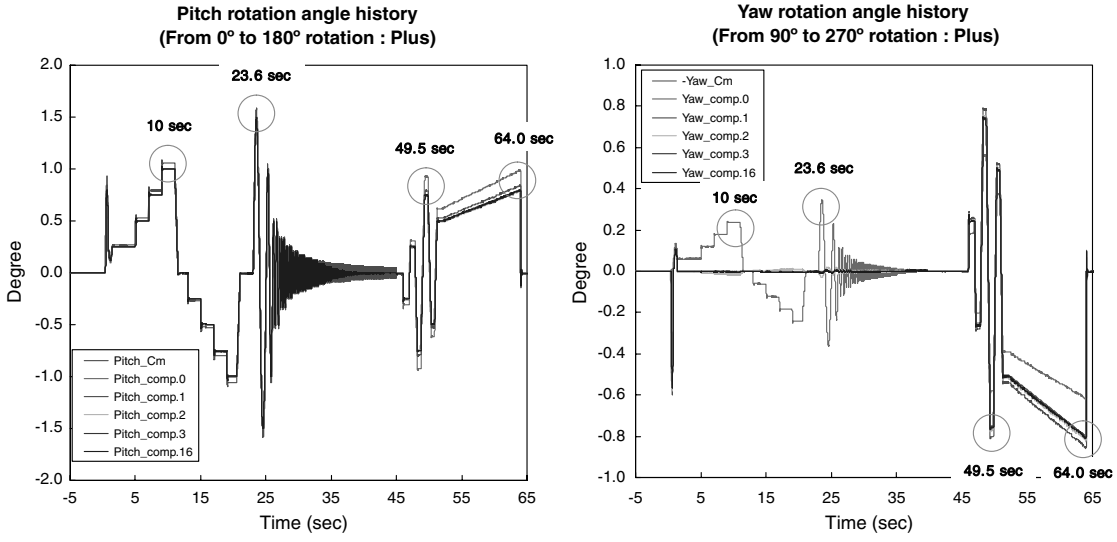

Fig. 9 Nozzle rotational angle history for TVC scenario test while varying iteration.

Table 4 Convergence of pitch rotational angle

	Step, 1.0 deg (10 s)		Sine, 1.5 deg (23.555 s)		Step, 0.75 deg (49.6 s)		Tilt, 0.8 deg (63.95 s)	
Iteration number	$\text{Pitch}_{\text{Comp}.i}$	$E_{ai.p}$ (%)	$\text{Pitch}_{\text{Comp}.i}$	$E_{ai.p}$ (%)	$\text{Pitch}_{\text{Comp}.i}$	$E_{ai.p}$ (%)	$\text{Pitch}_{\text{Comp}.i}$	$E_{ai.p}$ (%)
0	1.0018	——	1.5021	——	0.9311	——	0.9894	——
1	1.0582	5.335	1.5856	5.265	0.7927	17.458	0.8416	17.551
2	1.0009	5.729	1.4996	5.733	0.7394	7.208	0.7850	7.214
3	0.9977	0.324	1.4949	0.320	0.7473	1.060	0.7935	1.066
4	1.0010	0.328	1.4998	0.328	0.7504	0.407	0.7967	0.407
5	1.0011	0.018	1.5001	0.018	0.7499	0.060	0.7962	0.061
6	1.0010	0.019	1.4998	0.019	0.7497	0.023	0.7960	0.023
7	1.0009	0.001	1.4998	0.001	0.7498	0.003	0.7961	0.003
8	1.0010	0.001	1.4998	0.001	0.7498	0.001	0.7961	0.001
9	1.0010	$6.05E-05$	1.4998	$5.97E-05$	0.7498	$1.98E-04$	0.7961	$1.99E-04$
10	1.0010	$6.15E-05$	1.4998	$6.15E-05$	0.7498	$7.63E-05$	0.7961	$7.64E-05$
11	1.0010	$3.47E-06$	1.4998	$3.42E-06$	0.7498	$1.13E-05$	0.7961	$1.14E-05$
12	1.0010	$3.52E-06$	1.4998	$3.52E-06$	0.7498	$4.37E-06$	0.7961	$4.37E-06$
13	1.0010	$1.98E-07$	1.4998	$1.96E-07$	0.7498	$6.49E-07$	0.7961	$6.52E-07$
14	1.0010	$2.01E-07$	1.4998	$2.02E-07$	0.7498	$2.50E-07$	0.7961	$2.50E-07$
15	1.0010	$1.14E-08$	1.4998	$1.12E-08$	0.7498	$3.71E-08$	0.7961	$3.73E-08$
16	1.0010	$1.15E-08$	1.4998	$1.15E-08$	0.7498	$1.43E-08$	0.7961	$1.43E-08$

V. Convergence of Nozzle Rotational Angle

Figure 9 shows the convergence pattern of the nozzle rotational angle for iteration numbers 1, 2, 3, and 16. The four circles in Fig. 9 represented the highest nozzle rotational angle and the largest mismatches between the TVC command and the feedback at each step.

To evaluate the convergence of the nozzle rotational angle by increasing the iteration number, E_a (percent relative error) [9] is introduced next:

$$E_{ai.\text{pitch}} = \frac{\text{Pitch}_{\text{Comp}.i} - \text{Pitch}_{\text{Comp}.i-1}}{\text{Pitch}_{\text{Comp}.i}} \times 100;$$
$$E_{ai.\text{yaw}} = \frac{\text{Yaw}_{\text{Comp}.i} - \text{Yaw}_{\text{Comp}.i-1}}{\text{Yaw}_{\text{Comp}.i}} \times 100 \tag{5}$$

To evaluate the full step convergence, $E_{ai.\text{pitch}}$and $E_{ai.\text{yaw}}$ are calculated from the first to the 16th iteration at the four circle points in Fig. 9, as shown in Tables 4 and 5. After the 10th iteration, the pitch and yaw nozzle rotational angles have almost converged. Furthermore, to investigate the percent of relative errors during the full-test time at the 16th iteration, each history of $E_{ai.\text{pitch}}$ and $E_{ai.\text{yaw}}$ was calculated, as shown in Fig. 10. At the 16th iteration, the percent relative errors of the pitch and yaw angles were under 0.0004%. There are small errors in the pitch angle from 35 to 45 s, as shown in Fig. 10 (left-hand side). During this time, the pitch actuator moves the nozzle as $11 \sim 20$ Hz sine vibration. However, because the displacement data are acquired by analog 10 Hz low-pass filter (LPF), the small errors during this time can be generated by the analog LPF. The percent relative errors in yaw angle, as shown in Fig. 10 (right-hand side), are generated more significantly in the pitch-only actuation period than in the pitch and yaw simultaneous actuation. During the pitch-only actuation period, the angle of the yaw direction holds the neutrality, which is a very small rotational angle. When the pitch angle affects the neutral yaw angle in the pitch-only actuation period, because the relative change of the yaw angle is very large, the percent of relative error of the yaw angle is more significant in the pitch-only actuation period than in the pitch and yaw simultaneous actuation.

VI. Verification of Nozzle Rotational Angle Compensation and Thrust Vector Control Scenario Test

Before the ground firing test, the TVC scenario test (which is a TVC actuating test by the decided TVC scenario without combustion) is conducted for confirmation of the TVC performance. The largest actuating angle is ± 1.5 deg, the maximum actuating frequency is 20 Hz, and the pitch actuator moves only from 2 to 46 s in the TVC scenario, as shown in Fig. 8.

The nozzle displacements during the TVC scenario test are shown in Fig. 11. During the TVC scenario test, there is no translational

Table 5 Convergence of yaw rotational angle

	Neutrality, 0 deg (10 s)		Neutrality, 0 deg (23.555 s)		Step, −0.75 deg (49.6 s)		Tilt, −0.8 deg (63.95 s)	
Iteration number	$\text{Yaw}_{\text{Comp}.i}$	$E_{ai.y}$ (%)	$\text{Yaw}_{\text{Comp}.i}$	$E_{ai.y}$ (%)	$\text{Yaw}_{\text{Comp}.i}$	$E_{ai.y}$ (%)	$\text{Yaw}_{\text{Comp}.i}$	$E_{ai.y}$ (%)
0	0.2364	——	0.3496	——	−0.5795	——	−0.6186	——
1	−0.0037	6479.173	−0.0104	3452.497	−0.8026	27.803	−0.8557	27.712
2	−0.0172	78.501	−0.0304	65.740	−0.7695	4.311	−0.8203	4.316
3	−0.0035	393.369	−0.0098	209.611	−0.7567	1.688	−0.8067	1.682
4	−0.0027	28.482	−0.0087	13.186	−0.7586	0.250	−0.8087	0.251
5	−0.0035	22.438	−0.0099	11.956	−0.7593	0.096	−0.8095	0.096
6	−0.0036	1.249	−0.0099	0.660	−0.7592	0.014	−0.8094	0.014
7	−0.0035	1.285	−0.0099	0.684	−0.7592	0.006	−0.8093	0.005
8	−0.0035	0.072	−0.0099	0.038	−0.7592	0.001	−0.8094	0.001
9	−0.0035	0.074	−0.0099	0.039	−0.7592	$3.15E-04$	−0.8094	$3.14E-04$
10	−0.0035	0.004	−0.0099	0.002	−0.7592	$4.69E-05$	−0.8094	$4.70E-05$
11	−0.0035	0.004	−0.0099	0.002	−0.7592	$1.81E-05$	−0.8094	$1.80E-05$
12	−0.0035	$2.37E-04$	−0.0099	$1.25E-04$	−0.7592	$2.68E-06$	−0.8094	$2.69E-06$
13	−0.0035	$2.41E-04$	−0.0099	$1.28E-04$	−0.7592	$1.03E-06$	−0.8094	$1.03E-06$
14	−0.0035	$1.36E-05$	−0.0099	$7.13E-06$	−0.7592	$1.54E-07$	−0.8094	$1.54E-07$
15	−0.0035	$1.38E-05$	−0.0099	$7.35E-06$	−0.7592	$5.92E-08$	−0.8094	$5.90E-08$
16	−0.0035	$7.77E-07$	−0.0099	$4.08E-07$	−0.7592	$8.79E-09$	−0.8094	$8.80E-09$

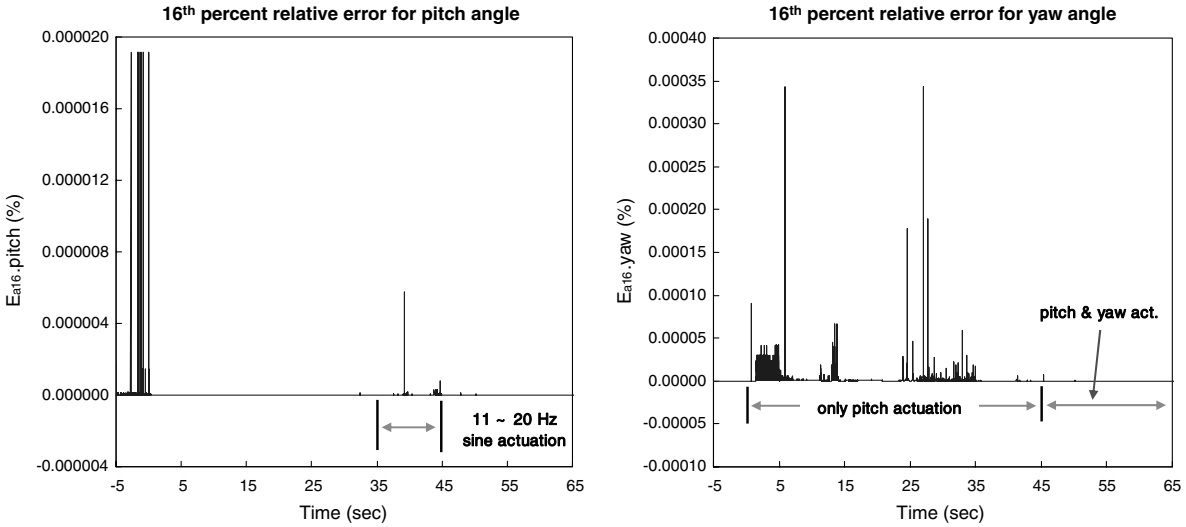

Fig. 10 Sixteenth percent relative error during TVC scenario test.

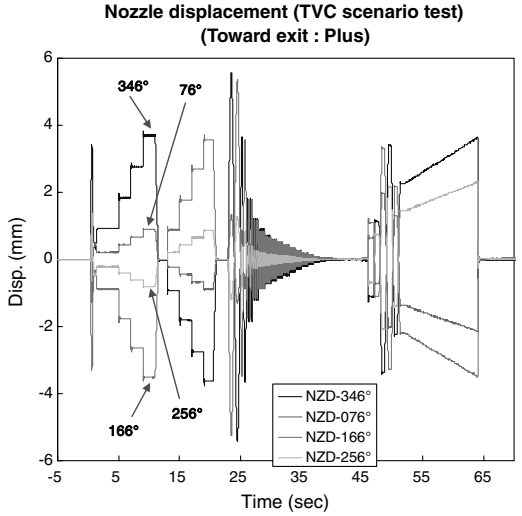

Fig. 11 Axial displacement for TVC scenario test.

motion but only rotational motion. The TVC actuator only generates the rotational motion of the nozzle. However, there is translation motion during the ground firing test because the nozzle moves toward the nozzle exit due to the combustion pressure.

Figure 12 shows the TVC scenario and the final compensated nozzle rotational angle history obtained by Eq. (4). Figures 13–16 show the expanded time views of the final compensated nozzle rotational angle history in the TVC scenario test. Overall, the yaw actuation error is slightly bigger than the pitch actuation error. Figure 15 shows the sine vibration period from 0.5 to 20 Hz. After 35 s (10 Hz sine vibration), the amplitude of the sine vibration rapidly decreases due to analog 10 Hz LPF, which is applied to avoid 60 Hz power source noise. When we see the yaw rotational angle history in Fig. 16, which is simultaneously the pitch and yaw actuation period, the amplitude is coincident with the yaw TVC command history, but the yaw rotational angle slightly shifts toward the 90 deg direction. This slight misalignment in the yaw direction is generated as the TVC actuator stroke setting procedure, which is not involved in the compensational logic for the offaxis effect of the TVC actuators. The TVC actuators are identically installed at 0 and 270 deg orthogonally. However, there are installation position errors generated by manufacturing and assembling errors of the TVC actuator support beam and TVC actuators. There is fairly good agreement between the TVC scenario and the nozzle rotational angle

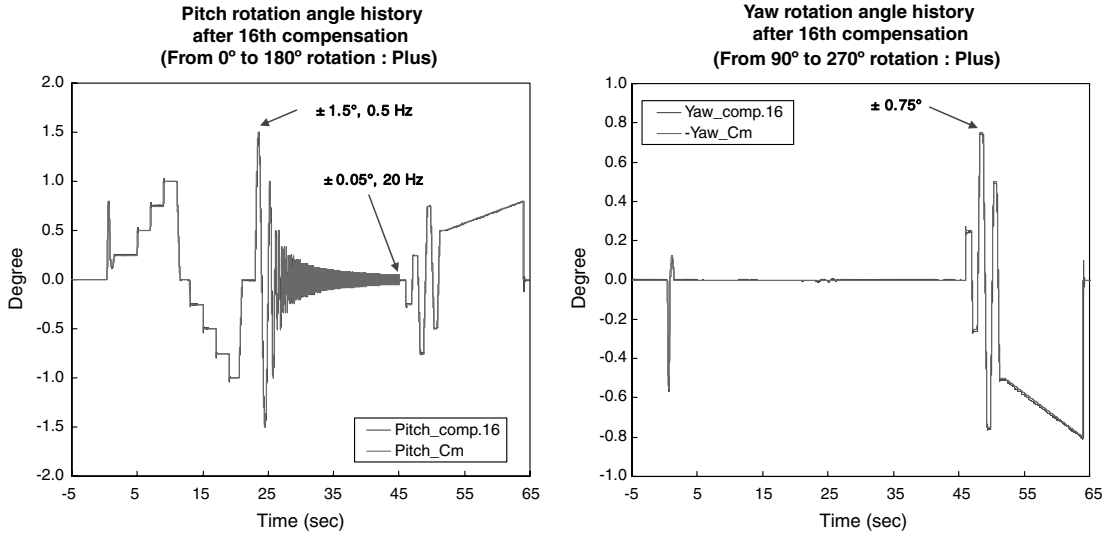

Fig. 12 Nozzle rotational angle history for TVC scenario test (after 16th compensation).

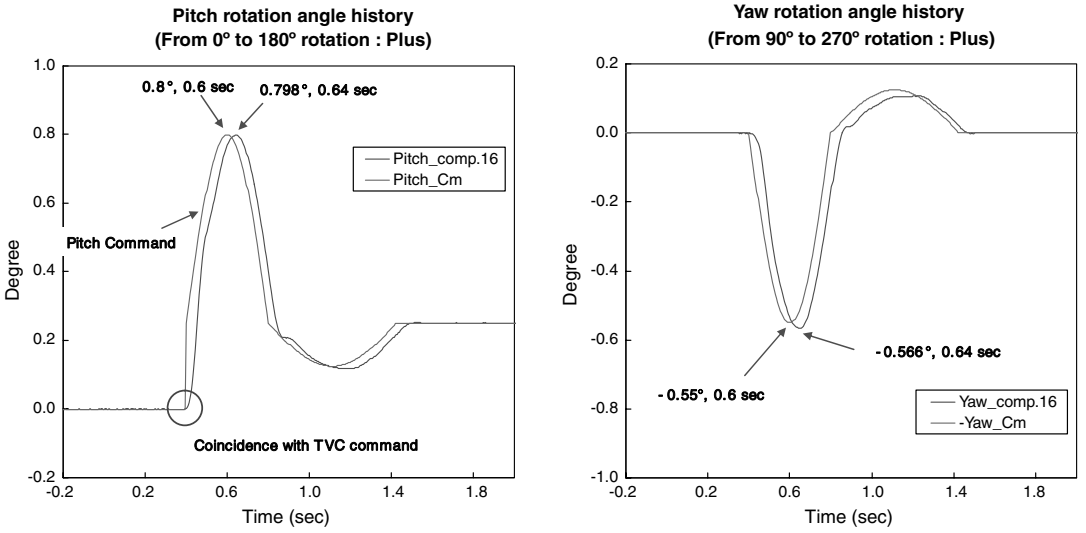

Fig. 13 Nozzle rotational angle history for TVC scenario test (−0.2 ∼ 2.0 s).

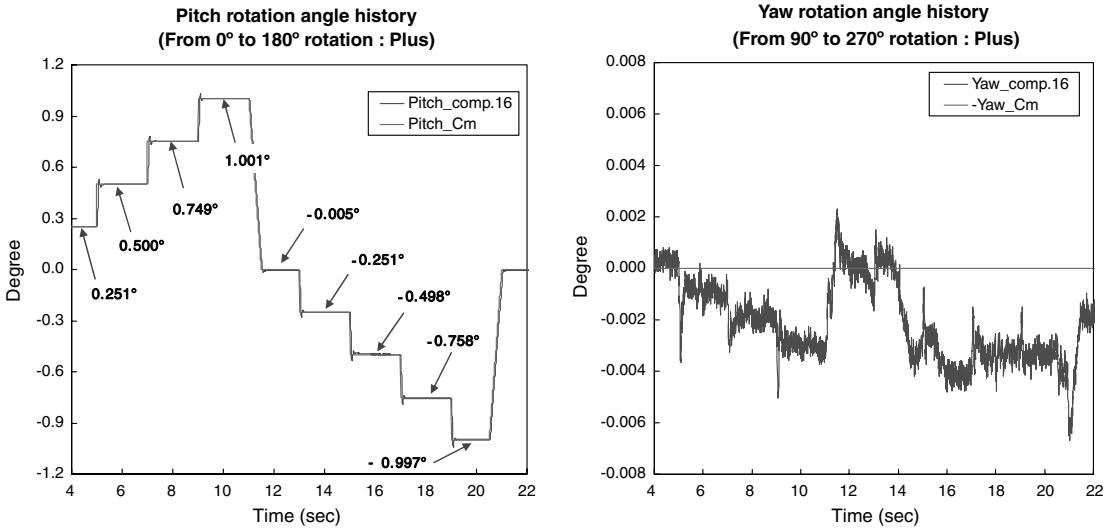

Fig. 14 Nozzle rotational angle history for TVC scenario test (4 ∼ 22 s).

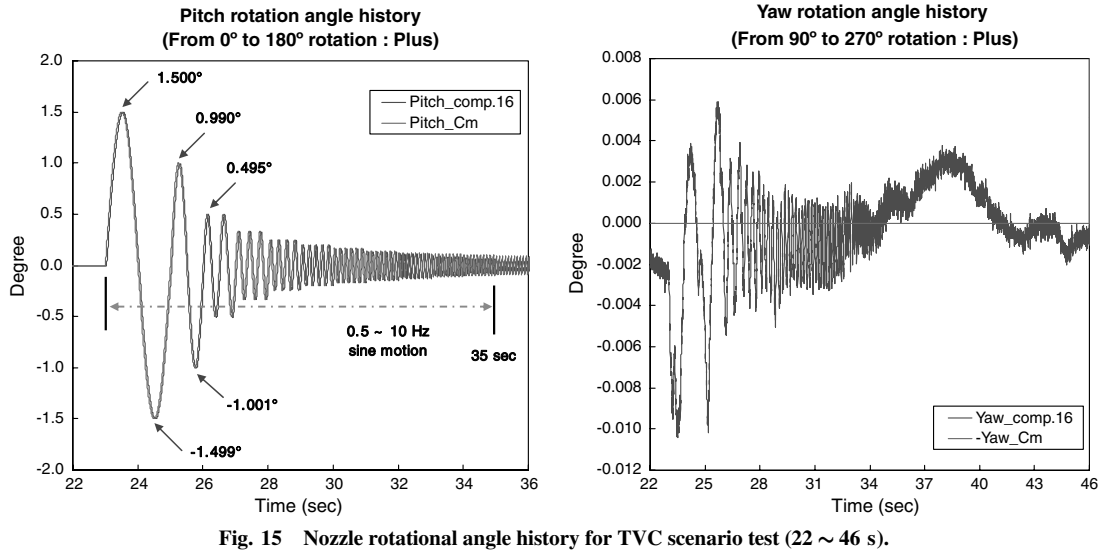

Fig. 15 Nozzle rotational angle history for TVC scenario test (22 ∼ 46 s).

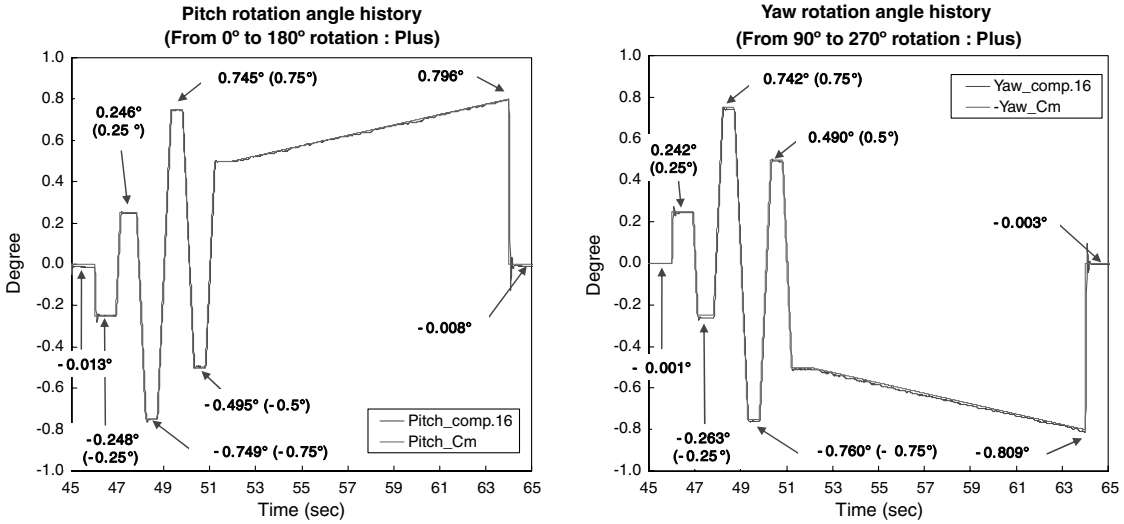

Fig. 16 Nozzle rotational angle history for TVC scenario test (45 ~ 65 s).

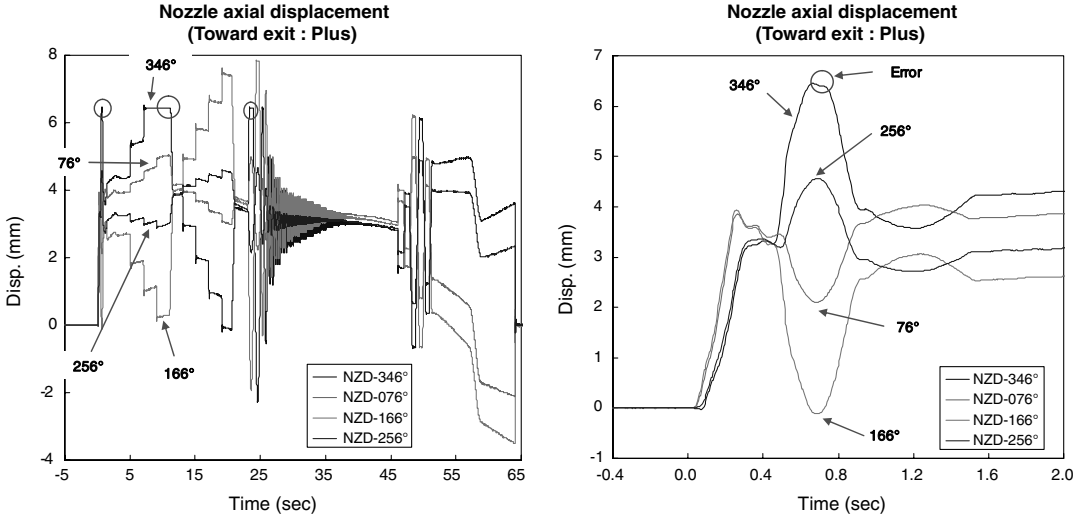

Fig. 17 GT No. 5 axial displacement history.

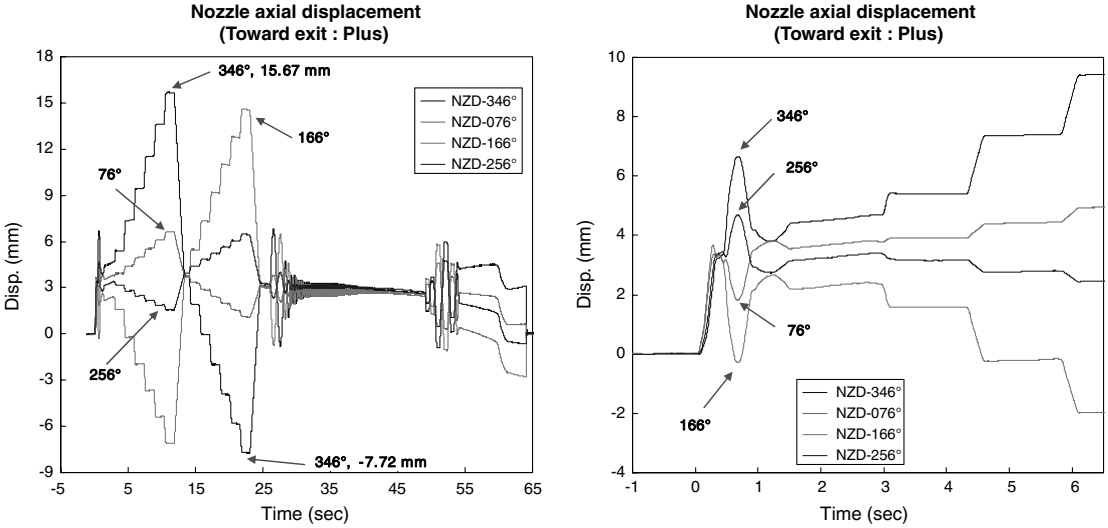

Fig. 18 GT No. 6 Axial displacement history.

within 0.01 deg, which means the deformation effect of the TVC support beam by the TVC actuating force is negligible to control the nozzle.

VII. Nozzle Motion on Ground Firing Test

Several TVC scenarios were designed to find the dynamic response limit and TVC control accuracy of the nozzle in the ground firing tests. The axial displacements of the nozzle induced by the combustion pressure were measured seven times for all the ground firing tests to confirm the margin of geometric interface and the effective stroke of the TVC actuator. Moreover, by the compensation equations for measured displacements, the nozzle rotational angle history was accurately estimated in the ground firing tests. In this paper, two important ground firing tests (GTs), which are GT No. 5 and GT No. 6, were represented.

A. Nozzle Axial Displacement History

The nozzle axial displacements during the ground firing tests are shown in Figs. 17 and 18. Figure 17 shows the nozzle axial displacement of GT No. 5, which represented the translational motion by the combustion pressure and the rotational motion by the GT No. 5 TVC scenario, as shown in Fig. 12. Because the counter potentiometer is not an active actuator but a pass position sensor, there is no resisting force against the nozzle axial displacement by the combustion pressure. Therefore (as shown in the right-hand side of Figs. 17 and 18), just after the ignition, the displacements at 76 and 166 deg, which are nearby the counter potentiometer, occur earlier than the displacements at 346 and 256 deg, which are nearby the TVC actuator.

For the GT No. 5 ground firing test, the displacement gauge installed at 346 deg cannot measure the nozzle displacement over 6.43 mm, in the neighborhood of 0.7, 10, and 23.7 s (which are marked in a circle in Fig. 17), due to the axial installation position error of the 346 deg displacement gauge. However, with the exception of the three circle regions in Fig. 17, the nozzle displacements are normally measured.

The GT No. 6 TVC scenario is similar to the GT No. 5, but the maximum nozzle rotational angle is 3 deg, which is two times the maximum angle of GT No. 5. When the nozzle rotates within ± 3 deg, the axial displacement of the 346 deg displacement gauge also moves from 15.67 to -7.72 mm during the ground firing test. The maximum moving stroke of the 346 deg displacement gauge is 23.39 mm. The 30 mm displacement gauge is sufficient to measure the ± 3 deg nozzle rotation during the ground firing test.

B. Nozzle Rotational Angle History

The nozzle rotational angle history of GT No. 5 is shown in Fig. 19. The nozzle rotational angle history also has errors in the

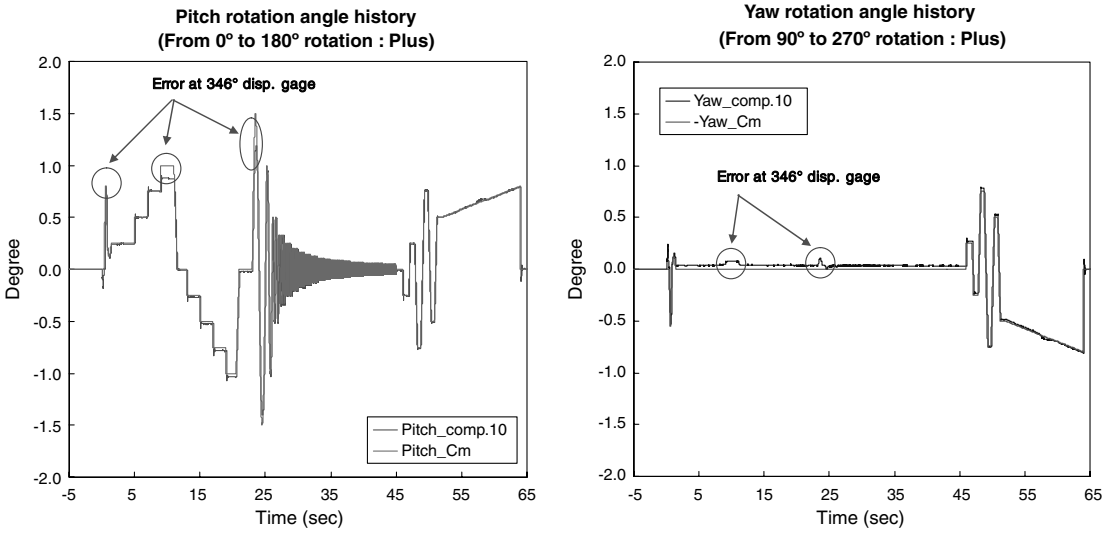

Fig. 19 GT No. 5 Nozzle rotational angle history.

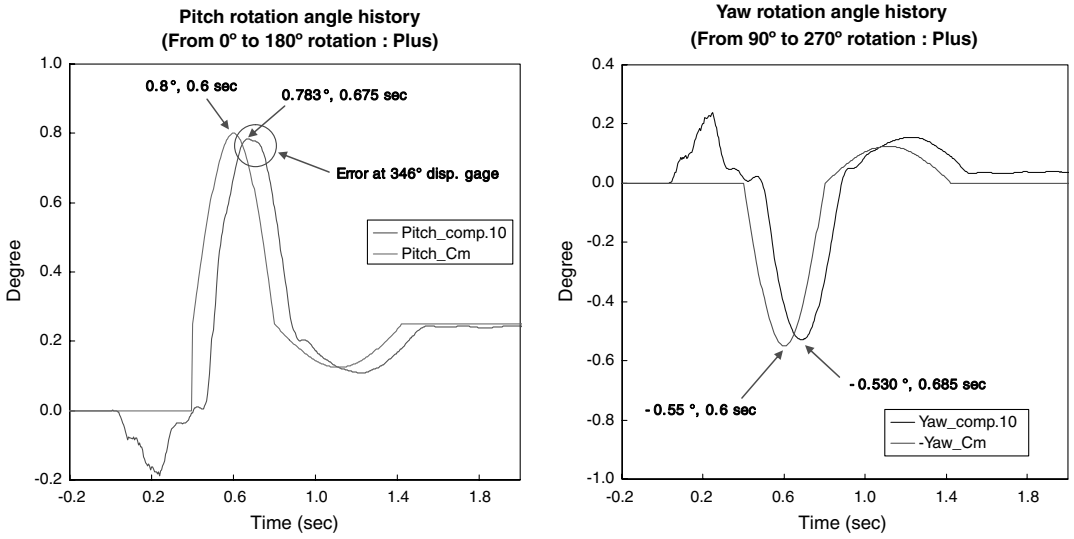

Fig. 20 GT No. 5 Nozzle rotational angle history ($-0.2 \sim 2.0$ s).

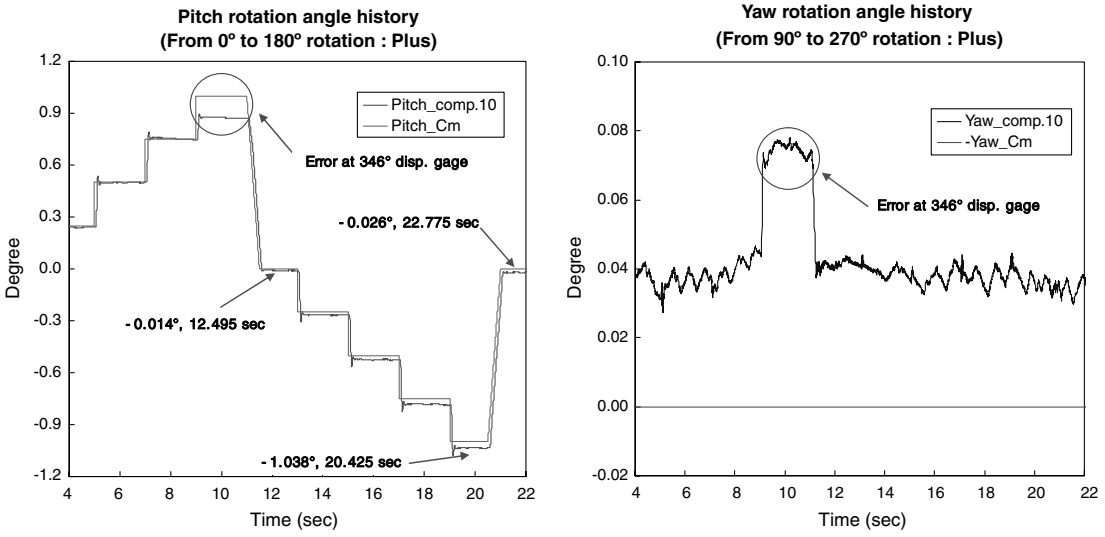

Fig. 21 GT No. 5 Nozzle rotational angle history (4 ∼ 22 s).

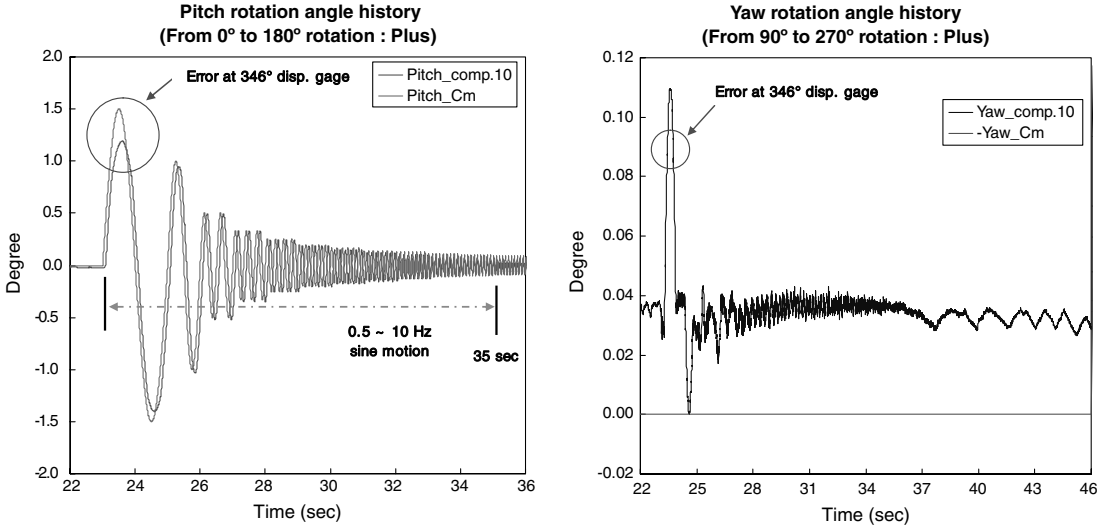

Fig. 22 GT No. 5 Nozzle rotational angle history (22 ∼ 46 s).

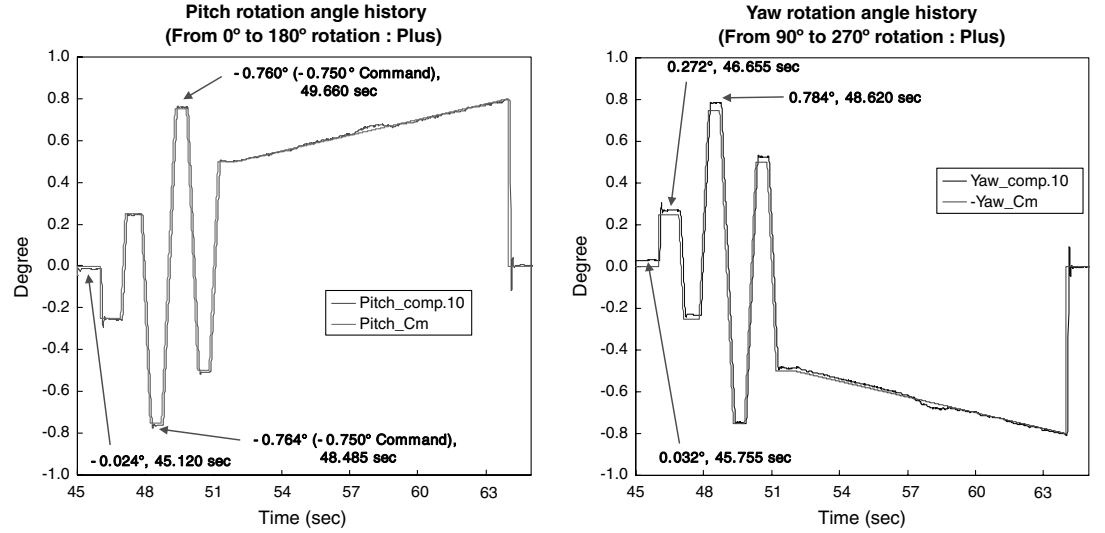

Fig. 23 GT No. 5 Nozzle rotational angle history (45 ∼ 65 s).

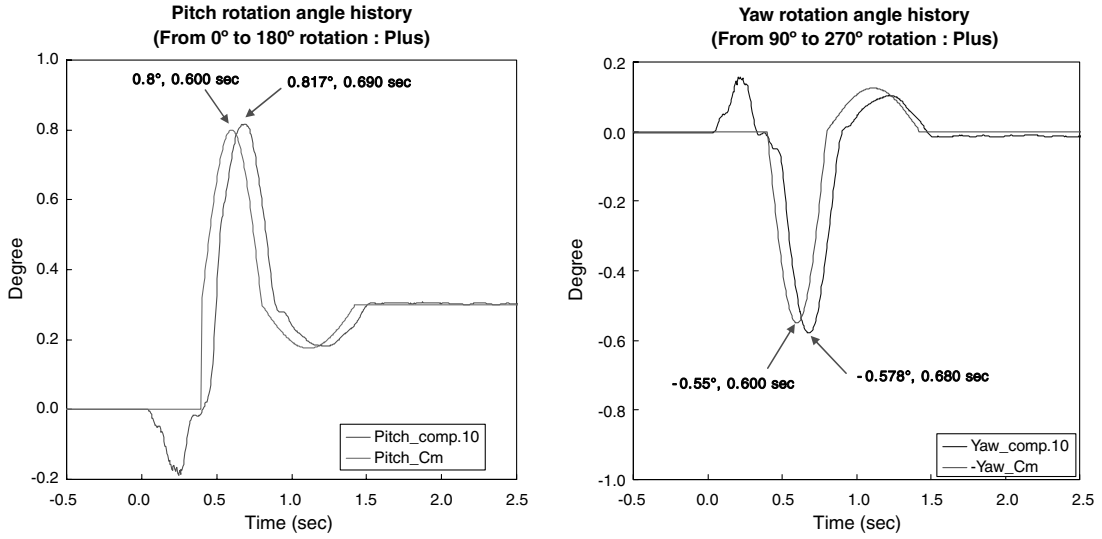

Fig. 24 GT No. 6 Nozzle rotational angle history ($-0.5 \sim 2.5$ s).

neighborhood of 0.7, 10, and 23.7 s, due to the measurement error of the 346 deg displacement gauge (as shown in Fig. 17). However, the nozzle rotational angle is measured normally in a major portion of the combustion time. Generally, the TVC actuators carry out the TVC command fairly. During most of the combustion time, there is about a 0.04 deg offset angle inclined toward the 270 deg (yaw) direction. There is also the maximum 0.026 deg offset angle inclined toward the 0 deg (pitch) direction in the TVC zero command maintenance period. This offset phenomenon is only generated in the ground firing test, but it is not generated in the TVC scenario test (as shown in Fig. 12). The offset phenomenon is related to the nonuniform deformation of the rear boss due to the combustion pressure, which makes the end position of the support beam move to the forward axial and inner radial direction nonuniformly (Fig. 2). The rear boss deformation was investigated two times in the kick motor hydropressure test [10].

Figures 20–23 show the expanded time views of the nozzle rotational angle history in GT No. 5. The maximum rotational angle and the offset quantity in the TVC zero command maintenance period are represented in each graph. The initial disturbance generated by the ignition shock, which is about 0.2 deg, is represented in Fig. 20 (GT No. 5) and Fig. 24 (GT No. 6). This initial ignition disturbance disappears within about 0.4 s. After this disturbance, the TVC actuator is able to control the kick motor by the decided TVC scenario. There is about $80 \sim 90$ ms time delay in comparison with the TVC command, as shown in Fig. 20 (GT No. 5) and Fig. 24 (GT No. 6) because of the nozzle damping effect. As shown in these figures, there is good agreement between the nozzle angle history and the TVC command within 0.04 deg.

The nozzle rotational angle history of GT No. 6 is shown in Fig. 25. During most of the combustion time, there is about a 0.038 deg offset angle inclined toward the 90 deg (yaw) direction (as shown in the right-hand side of Fig. 25) and the maximum 0.016 deg offset angle inclined toward the 180 deg (pitch) direction (as shown in Fig. 26) in the TVC zero command maintenance period, which represents the opposite offset angle direction in comparison with the offset angle direction of GT No. 5.

Figures 24 and 26–30 show the expanded time views of the nozzle rotational angle history in GT No. 6. The maximum rotational angle and the offset quantity in the TVC zero command maintenance period are represented in each graph. When the nozzle moves to ± 3 deg (as shown in Figs. 27 and 28), relatively large errors ($3.12 \sim -3.065$ deg) are generated because of the end position of the support beam deformation by the combustion pressure.

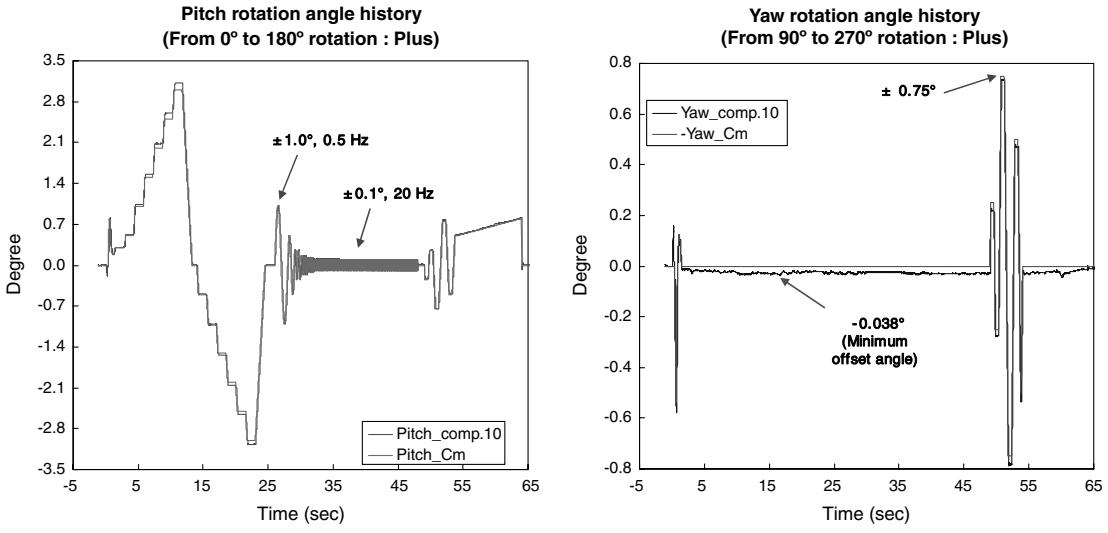

Fig. 25 GT No. 6 Nozzle rotational angle history.

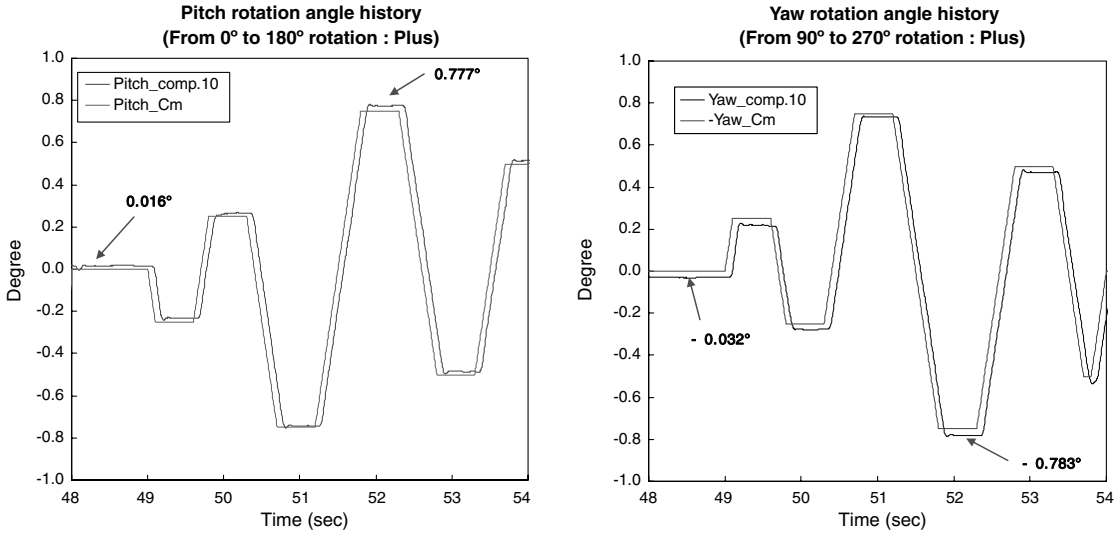

Fig. 26 GT No. 6 Nozzle rotational angle history (48 ∼ 54 s).

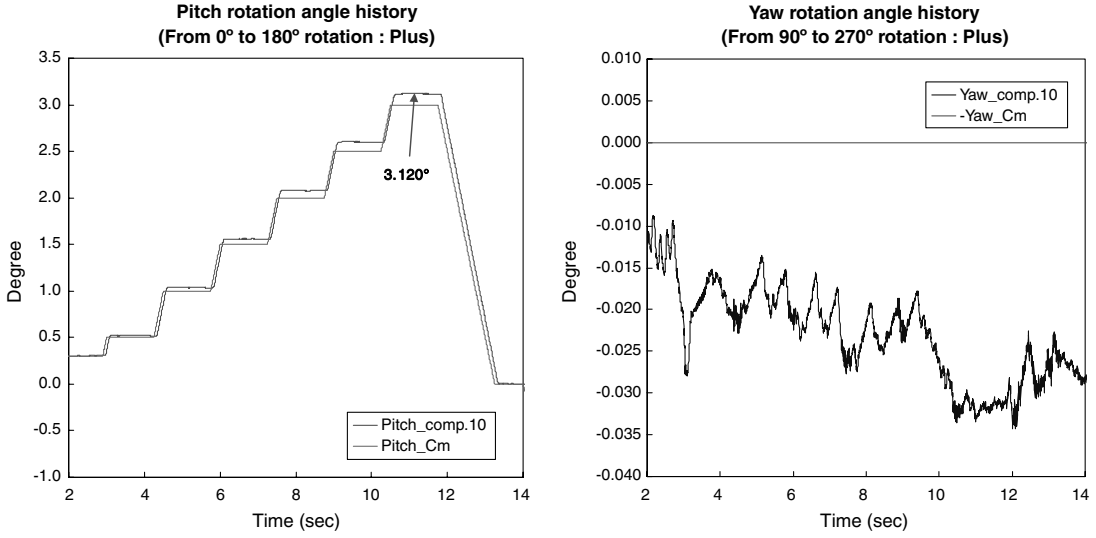

Fig. 27 GT No. 6 Nozzle rotational angle history (2 ∼ 14 s).

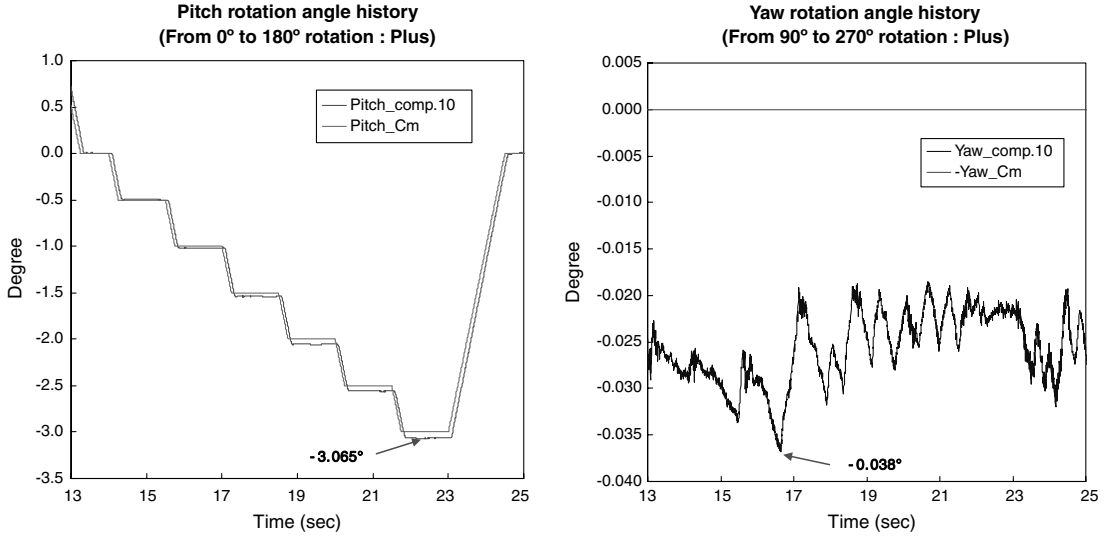

Fig. 28 GT No. 6 Nozzle rotational angle history (13 ∼ 25 s).

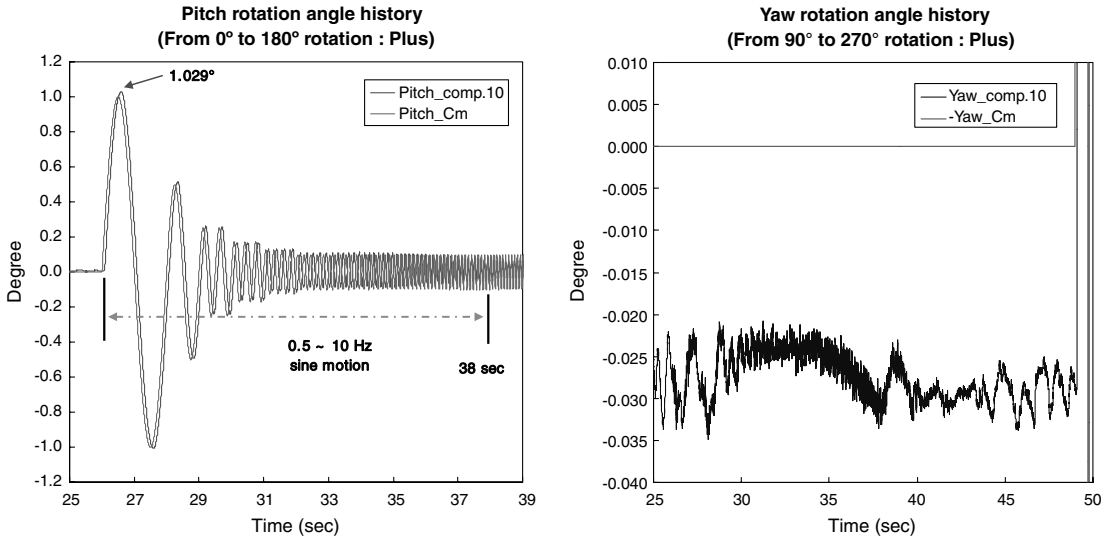

Fig. 29 GT No. 6 Nozzle rotational angle history (25 ∼ 50 s).

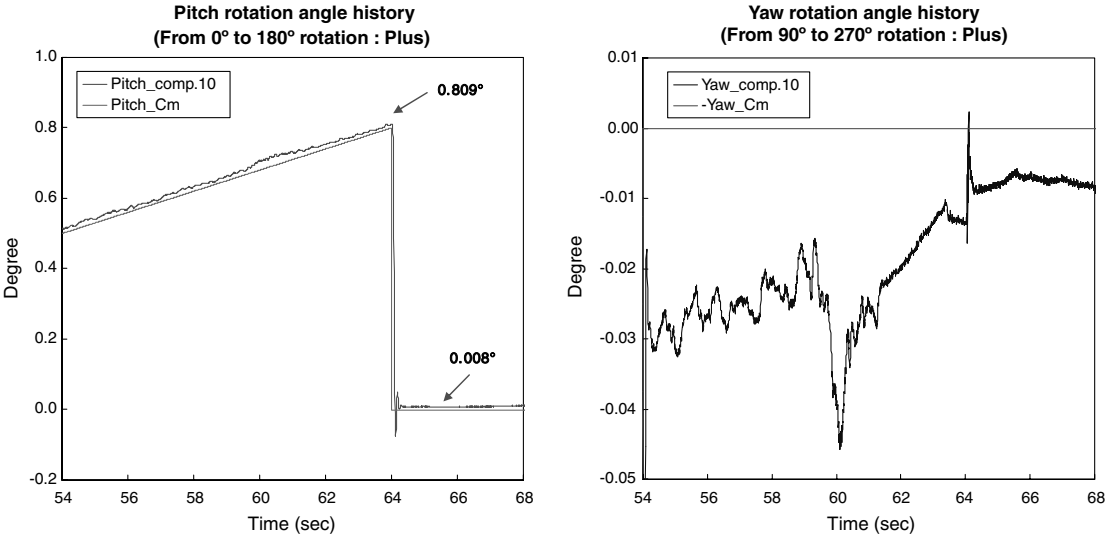

Fig. 30 GT No. 6 Nozzle rotational angle history (54 ∼ 70 s).

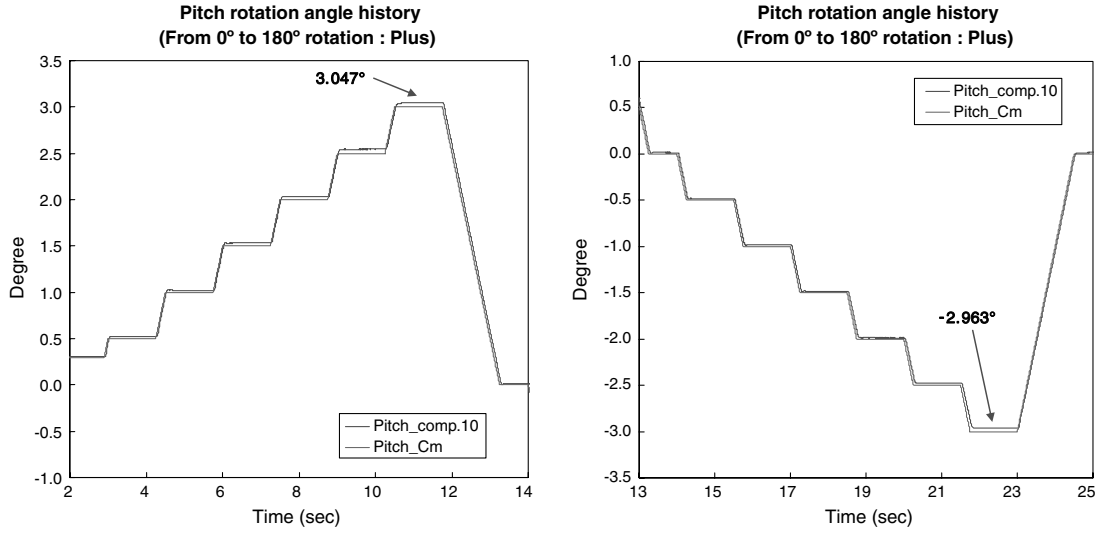

Fig. 31 GT No. 6 Nozzle pitch rotational angle history for TVC scenario test (2 ∼ 25 s).

However, in the TVC scenario test, in which there is no combustion pressure, there are relatively small errors ($3.047 \sim -2.963$ deg) (as shown in Fig. 31) in comparison with the ground firing test.

VIII. Conclusions

The nozzle displacement was measured by the displacement gauges. The nozzle rotational angle history was calculated by the measured displacements. A TVC stroke test was also done to get the linear coefficients for the compensation of the calculated nozzle rotational angle. In the TVC stroke test, the axial nozzle displacement and the inclinometer angle were measured simultaneously. The compensation of the calculated nozzle angle was done by the linear relation with the calculated nozzle angle and the inclinometer angle, with respect to the TVC input voltage.

However, when the TVC actuators move toward the pitch and yaw direction simultaneously, there is a couple effect between each displacement gauge. To compensate for this couple effect, the compensation equations are newly developed. The convergence of the nozzle rotational angle was also examined by varying the iteration number.

The nozzle rotational angle history in the TVC scenario test was obtained by the compensation of the calculated nozzle angle history from the measured displacement. In the TVC scenario test, there is fairly good agreement between the nozzle rotational angle history and the TVC command within 0.01 deg. Therefore, the deformation effect of the TVC support beam by the TVC actuation force is negligible to control the nozzle.

However, in the ground firing tests, there was an offset angle within the maximum 0.04 deg in the TVC zero command maintenance period because of the end position deformation of the support beam by the combustion pressure. The direction of the offset angle of the GT No. 5 and the GT No. 6 in the neutral position is not coincident.

When the nozzle moves to ± 3 deg in GT No. 6, the maximum TVC errors occurred as $3.12 \sim -3.065$ deg, which are larger than the TVC errors ($3.047 \sim -2.963$ deg) in the TVC scenario test.

The initial disturbance is generated by the ignition shock, which is about 0.2 deg. This initial ignition disturbance disappears within about 0.4 s. After this disturbance, the TVC actuator is able to control the kick motor by the decided TVC scenario. There is about a $80 \sim 90$ ms time delay in comparison with the TVC command because of the nozzle damping effect.

References

[1] Ishibashi, E., Okaya, S., Endo, T., and Ujino, T., "H-II-Solid Rocket Booster Thrust Vector Control System," AIAA Paper 95-2740, 1995.

[2] Gaffin, R. D., "Space Shuttle Solid Rocket Booster Nozzle Flexible Seal Pivot Point Dynamics," AIAA Paper 77-986, 1977.

[3] Ellis, R. A., "Supersonic Splitline (SSSL) Flexseal Nozzle Technology Evaluation Program," AIAA Paper 97-2721, July 1997.

[4] Akiba, R., Kohno, M., Inohara, H., Fujiwara, T., and Murakami, T., "Development of Movable Nozzle for Solid Rocket Motor," AIAA Paper 83-2285, Aug. 1983.

[5] Carnevale, C., and Resta, P. D., "Vega Electromechanical Thrust Vector Control Development," AIAA Paper 2007-5812, July 2007.

[6] Knauber, R. N., "Thrust Misalignments of Fixed-Nozzle Solid Rocket Motors," *Journal of Spacecraft and Rockets*, Vol. 33, No. 6, Nov.–Dec. 1996, pp. 794–799. doi:10.2514/3.26840

[7] Hamke, R., Rade, J., and Weldin, R., "Development and Qualification of a Star 48 Rocket Motor with Thrust Vector Control," AIAA Paper 92-3552, July 1992.

[8] Nagappa, R., Kurup, M. R., and Muthunayagam, A. E., "ISRO's Solid Rocket Motors," *Acta Astronautica*, Vol. 19, No. 8, 1989, pp. 681–697. doi:10.1016/0094-5765(89)90136-7

[9] Chapra, S. C., and Canale, R. P., "Approximations and Errors," *Numerical Methods for Engineers*, 2nd ed., McGraw–Hill, New York, 1990, p. 63.

[10] Yoo, J. S., and Kim, B. H., "Kick Motor Hydro Pressure Test," Korea Aerospace Research Institute Test Rep. 14535PA10000-003, Daejeon, Republic of Korea, 2006.

J. Martin
Associate Editor